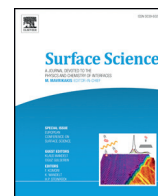




Contents lists available at ScienceDirect

Surface Science

journal homepage: www.elsevier.com/locate/susc

Interaction of carboxylic acids with rutile TiO₂(110): IR-investigations of terephthalic and benzoic acid adsorbed on a single crystal substrate

Maria Buchholz^a, Mingchun Xu^{b,c}, Heshmat Noei^{b,d}, Peter Weidler^a, Alexei Nefedov^a, Karin Fink^e, Yuemin Wang^{a,b,*}, Christof Wöll^{a,**}

^a Institute of Functional Interfaces, Karlsruhe Institute of Technology, 76021 Karlsruhe, Germany

^b Department of Physical Chemistry I and Laboratory of Industrial Chemistry, Ruhr-University Bochum, 44780 Bochum, Germany

^c School of Physics, Shandong University, 27 Shanda Nanlu, Jinan, Shandong 250100, P.R. China

^d Research Group X-ray Physics and Nanoscience, Deutsches Elektronen-Synchrotron DESY, Hamburg, Germany

^e Institute of Nanotechnology, Karlsruhe Institute of Technology, 76021 Karlsruhe, Germany

ARTICLE INFO

Available online xxxx

Keywords:

Carboxylic acids
Infrared spectroscopy
Terephthalic acid
Benzoic acid
Titanium oxide
DFT

ABSTRACT

The adsorption of two carboxylic acids, benzoic acid (BA) and terephthalic acid (TPA), on a single crystal rutile TiO₂(110) substrate was studied using infrared reflection–absorption spectroscopy (IRRAS) in conjunction with DFT calculations. On the basis of the high-quality IR data (in particular for the OH bands), various adsorbate species with different geometries could be identified. The adsorption of both, BA and TPA, on TiO₂(110) leads to deprotonation of carboxylic acids and protonation of substrate O-atoms. At low coverage, the deprotonated BA molecule adsorbs on TiO₂(110) in an upright, bidentate configuration, while the TPA molecule adopts a flat-lying geometry with both carboxylates bound to the surface in a monodentate geometry. At higher coverages, a transition from flat-lying to upright-oriented TPA molecules occurs. At saturation coverage, both BA and TPA molecules undergo dimerization indicating the presence of pronounced attractive intermolecular interactions. We propose that the BA dimers are stabilized by the interaction between adjacent phenyl rings, while the TPA dimerization is attributed to the formation of double hydrogen bonds between adjacent apical carboxylic groups.

© 2015 Elsevier B.V. All rights reserved.

1. Introduction

As a result of their catalytic, optical, and electronic properties, oxides are used in many application fields. A particular important example is titanium oxide which is used in catalysis and photocatalysis [1,2], as white pigment, in sun blockers, and also in solar technologies [3–5]. An important part of the Grätzel-cell, a dye-sensitized device for the conversion of sunlight into electrical energy (DSSC) first reported in 1991, is a mesoporous oxide layer (TiO₂, SnO₂, ZnO) [3]. Since the cross-section for photon absorption, the initial and crucial step in the conversion of light into electrical energy, is fairly small in bulk oxide materials, organic dye molecules are used in the Grätzel-cell as photon antennae. Photons absorbed by the organic molecule are converted into electron–hole (e–h) pairs. In the next step, the e–h pairs are transferred to the oxide where they are separated, and the conversion into electrical energy takes place. Typically, these dyes contain an aromatic core and are grafted to the TiO₂ surface via carboxylic acid groups reacting with

the surfaces of the TiO₂ particles yielding carboxylates bound to the substrate.

Titanium oxide exists in three different modifications: rutile, anatase, and brookite. Only the first two are used in technical applications. In the present work, we will focus on rutile, r-TiO₂, and in particular on its most stable (and thus most abundant) (110) surface. The chemical properties of this best-studied oxide surface, r-TiO₂(110), have been reviewed in quite some detail previously [6]. The surface chemistry of r-TiO₂(110) substrates is rather complex. Different preparation conditions, over-annealing or sputtering, leads to defects like oxygen vacancies which strongly influence the surface chemical properties. Whereas the fully oxidized surface is rather inert, at oxygen vacancies, a number of reactions become possible, rendering a defective oxide surface rather reactive [7].

In order to elucidate the chemical interaction of carboxylic groups with the r-TiO₂ substrate, the crucial step for anchoring dye molecules within a DSSC, we have undertaken a detailed investigation on the interaction of two simplest aromatic carboxylic acids, benzoic acid (BA) and terephthalic acid (TPA, often also referred to as benzenedicarboxylic acid (BDC)) with the rutile TiO₂(110) surface.

The adsorption of BA and TPA molecules on TiO₂ substrates has been extensively investigated in previous work. Guo et al. [8,9] studied the BA/TiO₂(110) model system by using scanning tunneling microscopy

* Corresponding author at: Institute of Functional Interfaces, Karlsruhe Institute of Technology, 76021 Karlsruhe, Germany.

** Corresponding author.

E-mail addresses: yuemin.wang@kit.edu (Y. Wang), christof.woell@kit.edu (C. Wöll).

(STM), electron stimulated desorption in ion angular distributions (ESDIAD), and low energy electron diffraction (LEED). They reported that BA adsorbs dissociatively on the $\text{TiO}_2(110)$ surface forming benzoate species, which are bound via the bidentate carboxylate groups to the five-fold coordinated Ti_{5c} atoms in an upright adsorption geometry. They proposed that the attractive interaction between adjacent benzoates results in the formation of T-shaped dimers along the $[1-10]$ direction. Further multiple investigations [10–12] using x-ray absorption spectroscopy (XAS), x-ray photoemission spectroscopy (XPS), and STM have confirmed these findings.

The adsorption of TPA molecules on $\text{TiO}_2(110)$ has also been studied by means of near-edge x-ray absorption fine structure (NEXAFS) spectroscopy, STM, and noncontact atomic force microscopy (NC-AFM) [13–16]. On the basis of the experimental results, the occurrence of two different adsorbate species was reported: at low coverages (up to 0.30 ML), the TPA molecules were found to adopt a disordered and flat-lying adsorption geometry, while at full monolayer, a conversion from a flat-lying to an upright orientation was detected (Fig. 1). In addition, the combined experimental and theoretical studies revealed dimerization of TPA molecules at saturation coverage [14–16].

Despite these efforts, more detailed information on the nature of the chemical anchoring of BA and TPA molecules to the r- $\text{TiO}_2(110)$ substrate is still lacking. This is mainly due to the fact that the experimental methods used so far (see above) are rather insensitive both to the deprotonation of BA and TPA molecules and also to the different configurations of carboxylate groups (e.g. mono- vs. bidentates). Further experimental and theoretical studies on BA/ TiO_2 and TPA/ TiO_2 systems are thus required to clarify the following points: 1) molecular vs. dissociative adsorption; 2) coverage-dependent adsorption structures; 3) origin of the dimer formation.

Here, we investigate the adsorption of BA and TPA molecules on $\text{TiO}_2(110)$ at different coverages by using infrared reflection-absorption spectroscopy (IRRAS). Determining the frequencies of the hydroxyl and carboxylate stretching bands with high resolution should allow for unambiguous conclusions on the question whether carboxylic acid groups are still intact or are deprotonated upon interaction with the substrate. If the acid is deprotonated, a substrate hydroxyl species should be formed, exhibiting a characteristic vibrational frequency clearly different from vibrations of a carboxylic acid group. In addition, a close analysis of the IR data allows us to gain deeper insight into the adsorption configuration (i.e. the occurrence of mono- and bidentate species) and into the question whether dimers of BA and TPA adsorbate species are present on $\text{TiO}_2(110)$. This question is particularly interesting in case of TPA, since for an upright species (as proposed in previous works [13–16]), one would assume the occurrence of both protonated and deprotonated carboxylic acid groups.

In the past, the acquisition of high-resolution IRRAS data recorded at grazing incidence for dielectric single crystals has only very rarely been reported due to technical difficulties. In this work, high-quality IRRAS data (showing, in particular, well-resolved substrate hydroxyl bands) are reported which provide direct spectroscopic evidence for the formation of different coverage-dependent adsorption species after exposure of the $\text{TiO}_2(110)$ surface to BA and TPA molecules. The assignment of the experimentally observed vibrational bands is supported by DFT calculations.

2. Experimental

2.1. IRRAS experiments

All IRRAS spectra presented here were recorded using a novel UHV-FTIR apparatus (Prevac, Rógow, Poland) [17] equipped with a state-of-the-art FTIR spectrometer (Bruker Vertex 80v, Bruker Optics, Ettlingen, Germany). The r- $\text{TiO}_2(110)$ single crystal (10×5 mm, MaTeck, Jülich, Germany) was prepared by a sequence of sputtering and annealing cycles as described in Ref. [7]. The BA and TPA molecules (purchased from Merck and Aldrich and used without further processing) were deposited on the substrate by employing a Knudsen cell evaporator in a dedicated preparation chamber, which is connected via a distribution chamber to the infrared chamber of the apparatus. The vapor pressure of benzoic acid was sufficiently high to also obtain deposition for a room temperature Knudsen cell. The thick layer was prepared by exposing the cold substrate (140 K) to the molecular beam originating from the Knudsen cell. In case of TPA, the vapor pressure is so small that with a room temperature Knudsen cell only submonolayers could be prepared. For higher coverages, the Knudsen cell containing TPA molecules had to be heated to 433 K to obtain a flux sufficiently intense for the preparation of TPA mono- and multilayers.

The high-resolution IR spectra reported here were taken with a base pressure in the IR chamber of $1 \cdot 10^{-10}$ mbar. A grazing angle of incidence angle of 80° was used. For each set of data, 2048 scans with a resolution of 4 cm^{-1} were accumulated. Background correction was carried out by subtracting a reference spectrum recorded using the same parameters for the clean substrate immediately before deposition of the molecular adsorbates.

IR-reflectivity and -absorbance calculations were performed by using the equations derived by Hansen et al. [18,19] and by Mielczarski et al. [20], as described in detail in Ref. [21].

2.2. DFT calculations

All quantum chemical calculations have been performed with the plane wave code VASP [22,23]. The $\text{TiO}_2(110)$ surface was treated in

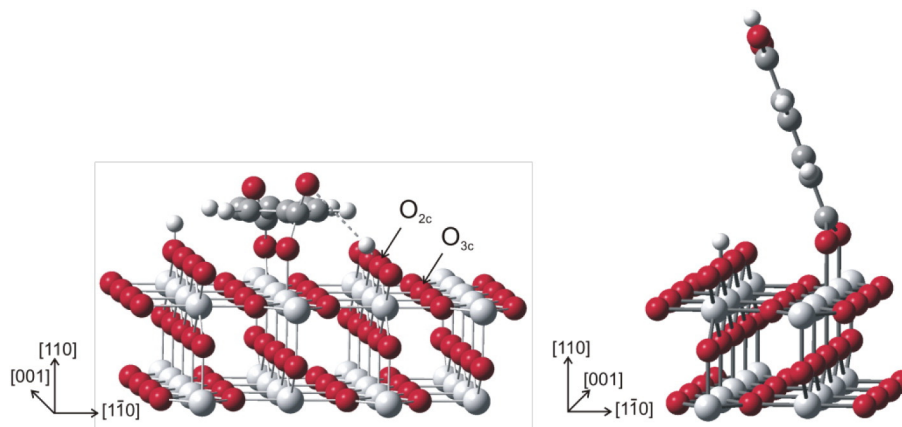


Fig. 1. Ball-stick model for the adsorption of terephthalic acid on rutile $\text{TiO}_2(110)$. Left panel: flat-lying configuration, right panel: upright configuration [13,16]. Color code: oxygen (TPA) = red, carbon = grey, hydrogen = white, oxygen (TiO_2) = red, titanium = light grey.

the same way as in Ref. [7], i.e. a 6×2 surface cell was used. Along the z-direction four Ti layers and the corresponding O layers were taken into account. The total extension in z-direction amounted to 25 Å, which corresponds to a vacuum layer of 12 Å. This fairly large vacuum layer thickness is necessary to make sure that the adsorbed molecules do not interact with the next slab.

In all calculations, the gradient corrected PBE functional [24] was used in connection with the projector augmented wave potentials PAWs [23,25] and an energy cutoff of 400 eV. Starting from the bulk structure, the positions of the ions of the upper two O–Ti–O layers were optimized. Then the deprotonated carboxylic acid was positioned in such a way on the surface that the two O ions of the carboxylate group were bound to surface Ti_{5c} ions. In the subsequent structure optimization, the atoms of the organic molecule as well as the two Ti adsorption sites and all surface O_{2c} ions were considered. The vibrational frequencies were calculated numerically; here, two displacements of all of the atoms of the organic molecule as well as the two Ti adsorption sites in each direction were considered.

3. Results

3.1. Adsorption of benzoic acid on rutile $TiO_2(110)$

Fig. 2 displays the IRRAS data recorded after adsorption of benzoic acid (BA) on r- $TiO_2(110)$ at different temperatures. For the spectra obtained at room temperature (curves A, B), only two absorbance bands were observed at the low-frequency region, one positive at 1498 cm^{-1} and one negative at 1426 cm^{-1} . The spectrum obtained after BA adsorption at 140 K (curve C) is more complex. A large number of bands are observed at 1701 , 1602 , 1585 cm^{-1} , 1495 , 1455 , 1425 , 1327 , and 1301 cm^{-1} . Among them, the 1701 cm^{-1} band is the dominating one. The intensity of these peaks is increasing with increasing dosage, revealing the formation of BA multilayer at 140 K, while at room temperature, only the monolayer adsorption of BA on $TiO_2(110)$ is observed. Based

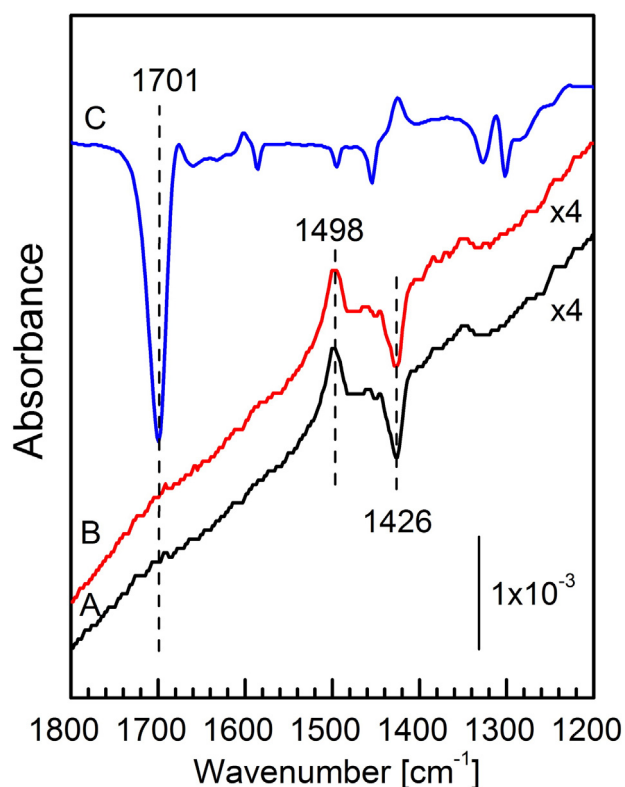


Fig. 2. IRRAS spectra of benzoic acid (BA) on rutile $TiO_2(110)$ at different coverages. (A) submonolayer, (B) full monolayer, (C) multilayer.

on the IR data reported for BA in condensed phase [26], the multilayer-related IR bands can be assigned to the different vibrational modes. All the frequencies and mode assignments are summarized in Table 1. Note that the phenyl ring modes are described in terms of Wilson notation [27].

For the monolayer adsorption of BA, the two dominating bands at 1426 and 1498 cm^{-1} are characteristic for the carboxylate species formed via deprotonation of BA and are assigned to the symmetric $\nu_s(\text{OCO})$ and asymmetric $\nu_{as}(\text{OCO})$ stretching vibrations, respectively. In addition, the small frequency splitting of 72 cm^{-1} reveals that BA is bound to the surface via a bidentate carboxylate group, as supported by DFT calculations shown below. The dissociative adsorption of benzoic acid on $TiO_2(110)$ is further supported by the absence of a $\nu(\text{C}=\text{O})$ band around 1700 cm^{-1} originating from the molecular adsorption of BA.

Importantly, the observation of OH bands (Fig. 3) provides direct evidence for the deprotonation of benzoic acid on $TiO_2(110)$. For submonolayer adsorption (Fig. 3A–C), two OH bands at 3700 and 3622 cm^{-1} were detected, while at saturation coverage (Fig. 3D), only the 3700 cm^{-1} band is visible. A closer analysis of the IR data will be given in the Section 4.

3.2. Adsorption of terephthalic acid on rutile $TiO_2(110)$

Fig. 4 shows the IRRAS data recorded after terephthalic acid (TPA) adsorption at room temperature on the rutile $TiO_2(110)$ at different coverages. At low coverage (Fig. 4A, B), we find two C–O stretching vibrations at 1412 and 1635 cm^{-1} . Upon increasing the TPA dose, the IR spectra show new bands at 1427 , 1498 , and 1760 cm^{-1} (Fig. 4C), which differ substantially from the data at low coverages. At full monolayer, a new band appears at 1690 cm^{-1} . Further exposure to TPA leads to the appearance of a number of IR bands at 1713 , 1682 , 1576 , 1511 , 1422 , 1320 , and 1290 cm^{-1} (Fig. 4E). They are characteristic for the formation of multilayer TPA, in good agreement with the data seen in the corresponding IR spectra of solid TPA [28]. The mode assignments of the observed IR bands are summarized in Table 1 and will be further discussed in Section 4.

Important results are shown in the hydroxyl region of the IR spectra (Fig. 5). The vibrations in this region allow to determine if the TPA is still protonated or deprotonated on the surface. At low coverage, one single OH band was observed at 3700 cm^{-1} (Fig. 5B). With increasing the TPA coverage, two new OH bands show up at 3621 and 3582 cm^{-1} (Fig. 5C). At full monolayer (Fig. 5D) the intensity of the 3582 cm^{-1} band is clearly decreased, while the OH bands at 3700 and 3622 cm^{-1} remain nearly unchanged in intensity. The observation of different OH bands indicates

Table 1

Frequencies [cm^{-1}] and mode assignments for submonolayer (subML), full monolayer (ML), and multilayer (MultiL) adsorption of BA and TPA molecules on $TiO_2(110)$. For comparison, the results of DFT calculations are also shown (ν : stretching; δ : in-plane bending).

BA		TPA			Assignments ^b		
DFT	MultiL ^a	ML	DFT	MultiL ^a	ML	subML	
	1701		1732	1713	1760	$\nu(\text{C}=\text{O})$	
				1682	1690	$\nu(\text{C}=\text{O})$	
	1602		1603			$\nu(\text{CC})_{\text{ring}}$, 8a	
	1585		1568	1576		$\nu(\text{CC})_{\text{ring}}$, 8b	
	1495		1481	1511		$\nu(\text{CC})_{\text{ring}} + \delta(\text{CH})$, 19a	
1452		1498	1441		1498	1635	$\nu_{as}(\text{OCO})$
	1455			1422			$\delta(\text{CH}) + \nu(\text{CC})_{\text{ring}}$, 19b
	1425						
1409		1426	1363		1427	1412	$\nu_s(\text{OCO})$
1383							
1358	1327		1327	1320			$\nu(\text{CC})_{\text{ring}} + \delta(\text{CH})$, 14
1299	1301			1290			$\delta(\text{COH}) + \nu(\text{C}-\text{O})$

^a The assignments of multilayer-related modes are based on the IR data of solid BA [26] and TPA [28].

^b The vibrational modes of phenyl rings are described in terms of Wilson notation [27].

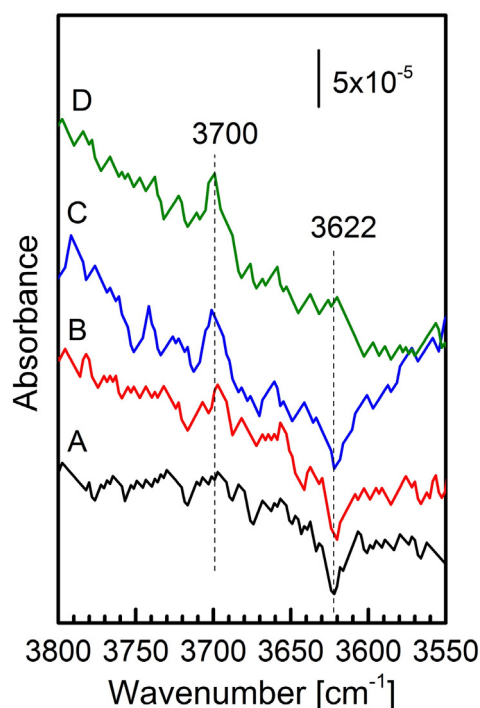


Fig. 3. Hydroxyl region of IRRA spectra of benzoic acid (BA) on rutile $\text{TiO}_2(110)$. The substrate was exposed to different amounts of BA at room temperature: (A) 0.09 L, (B) 0.18 L, (C) 0.36 L, and (D) 1.44 L.

the presence of various TPA species depending on the coverage, as discussed in detail in Section 4.

3.3. DFT calculations

In all calculations, adsorption of the deprotonated carboxylic acids in an upright position was assumed. For the remaining proton, the adsorption at O_{2c} and O_{3c} sites was investigated. The binding to O_{2c} was found to be 2.5 eV more stable than to O_{3c} . The calculated OH frequencies are 3795 cm^{-1} for O_{2c} and 3614 cm^{-1} for O_{3c} , respectively. The difference between the two OH frequencies amounts to 181 cm^{-1} . For the numerical calculations of the OH frequencies, only the movements of the involved O and H atoms have been considered. In particular for the more flexible O_{2c} position, this approximation can cause an uncertainty in the frequency.

As expected, the adsorbed carboxylic groups of BA and TPA show similar vibrational frequencies. We observed the symmetric stretching $\nu_s(\text{OCO})$ at 1383 cm^{-1} for BA and 1363 cm^{-1} for TPA. For the asymmetric stretching $\nu_{as}(\text{OCO})$, higher frequencies of 1452 cm^{-1} (BA) and 1441 cm^{-1} (TPA) were obtained. BA shows an additional vibration with contributions of the COO^- group at 1409 cm^{-1} . In our calculations, the carbonyl stretching vibration $\nu(\text{C}=\text{O})$ of the COOH group in TPA is found at 1730 cm^{-1} and the bending mode of the COH group at 1327 cm^{-1} .

A dianionic form of TPA was energetically 2.5 eV less favorable than the monoionic one. For the dianionic configuration, the first frequencies below the C–H stretching bands are ring vibrations starting at 1600 cm^{-1} , the asymmetric stretching mode $\nu_{as}(\text{OCO})$ of the upper COO^- group is found at 1470 cm^{-1} . The bands at 1405 cm^{-1} and 1344 cm^{-1} are linear combinations of the symmetric $\nu_s(\text{OCO})$ of both carboxylate groups.

4. Discussion

To gain deeper insight into the adsorption geometry of BA and TPA on $\text{TiO}_2(110)$, a detailed analysis of the interaction between the incident

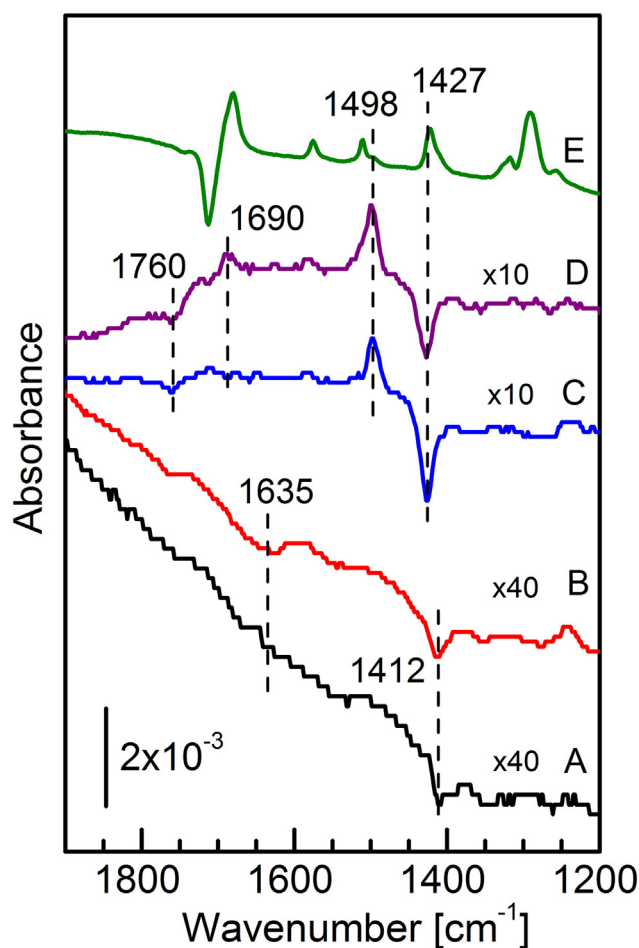


Fig. 4. IRRA spectra of terephthalic acid (TPA) on rutile $\text{TiO}_2(110)$ at different coverages. (A, B) submonolayer, (C, D) monolayer, (E) multilayer.

light and adsorbate-related vibrations is required. When applying IRRAS to characterize molecular adsorbates on metal surfaces, the so-called surface selection rule has to be considered: Only vibrational modes with a transition dipole moment (TDM) orientated perpendicular to the surface can be excited by p-polarized light resulting in a reduction in reflectivity (positive absorbance bands). In contrast to metal surfaces, for dielectrics (oxides), the situation is much more complex. Both s- and p-polarized components of the incident light can couple to adsorbate vibrations (Fig. 6). The sign of the vibrational signals on dielectric materials can be explained by the reflectivity calculations described in Refs. [18–21,29]. The s-polarized light is oriented parallel to the surface and perpendicular to the incidence direction (Fig. 6A). The absorbance bands excited by s-polarized light (E_s) are always negative. For p-polarized light, it is more complicated, the electric field can be orientated parallel to the surface (tangential p-polarized light $E_{p,t}$) and normal to the surface (normal p-polarized light $E_{p,n}$). The IRRAS bands excited by p-polarized light can be negative or positive depending on the incidence angle θ and the refractive index n of the substrate (see Fig. 6B). The $E_{p,n}$ component couples only to vibrations with a component of the TDM perpendicular to the surface. The component of the TDM parallel to the surface can be excited either by E_s or by $E_{p,t}$ component, depending on the azimuth orientation.

Since the carboxylate-related IRRAS bands are either negative (increase in reflectivity) or positive (decrease in reflectivity), we have calculated the reflectivity differences ($\Delta R = R_0 - R_a$) between the clean (R_0) and adsorbate-covered (R_a) $r\text{-TiO}_2(110)$ substrates as a function of incidence angle θ for both 1426 cm^{-1} and 1498 cm^{-1} frequencies. They show the similar ΔR curves (Fig. 6B). For an incidence of 80° , like

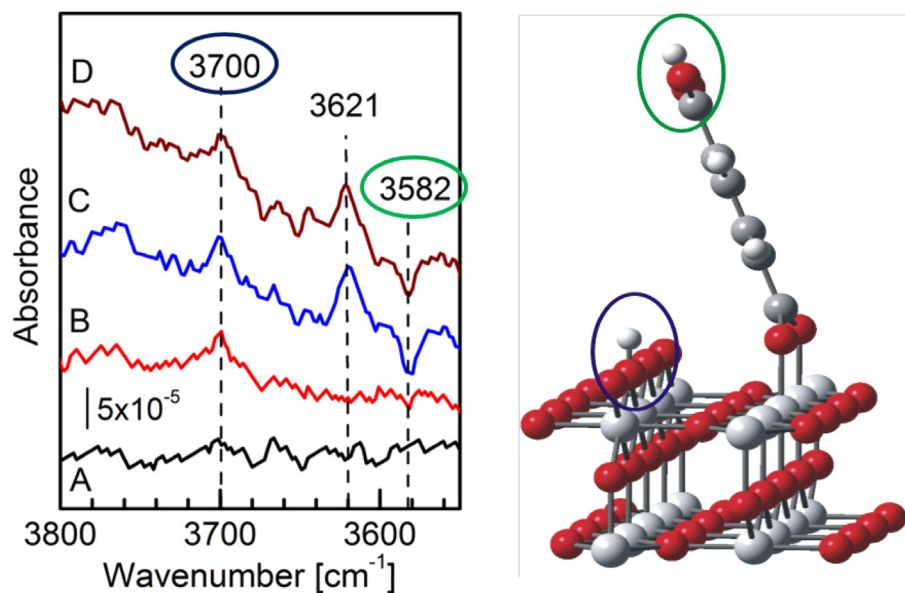


Fig. 5. Hydroxyl region of IRRA spectra of terephthalic acid (TPA) on rutile TiO_2 (110) with increasing coverages. (A, B) submonolayer, (C, D) monolayer.

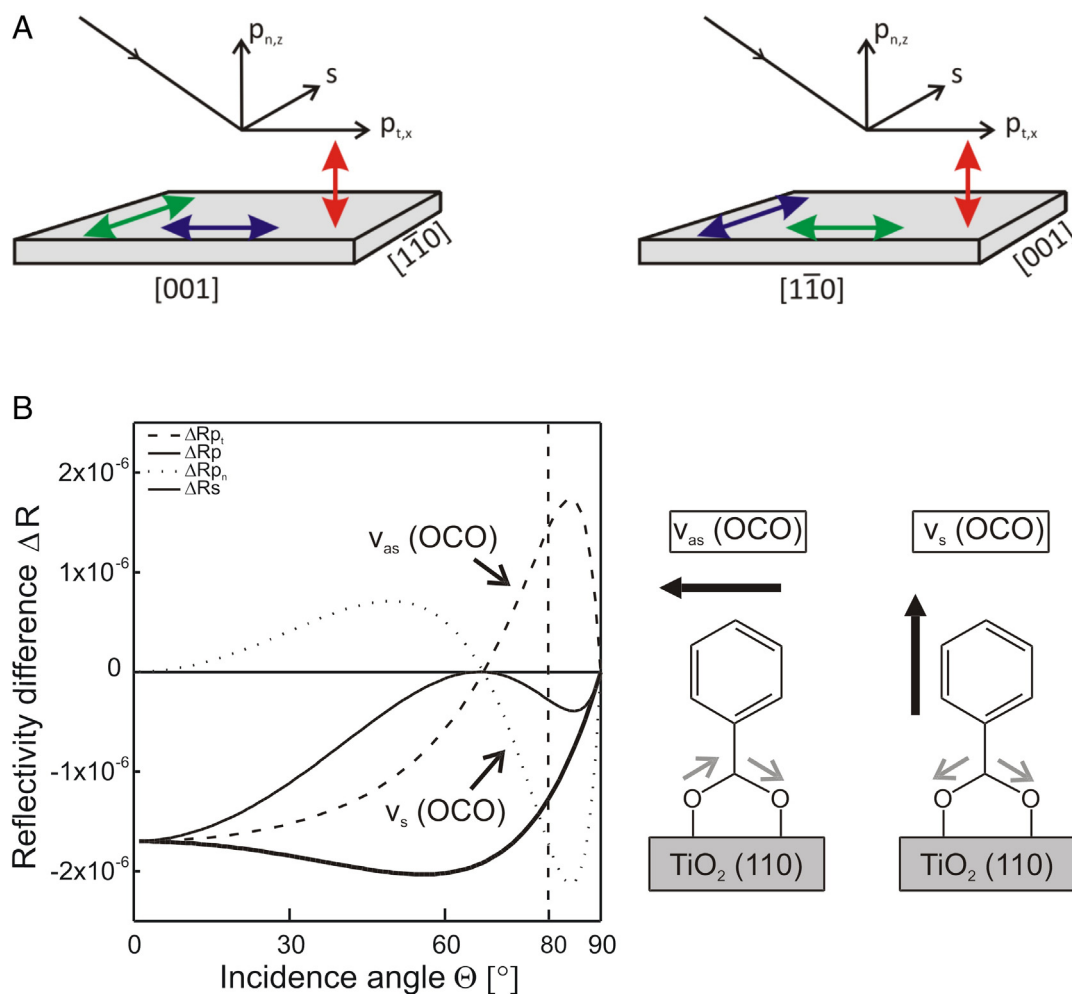


Fig. 6. A) Orientation of the s- and p-polarized components for the incident light along [001] (left) and $[1\bar{1}0]$ azimuth (right). B) Left panel: Calculated reflectivity differences ($\Delta R = R_0 - R_s$) between the clean (R_0) and BA covered (R_s) $r\text{-TiO}_2(110)$ substrates as a function of incidence angle for p-polarized (x- and z-component (dashed lines) and sum (solid line)) and for s-polarized (bold solid line) light at 1425 cm^{-1} . The following optical constants were used [29]: refractive index $n_3 = 2.4$, extinction coefficient $k_3 = 0$, $n_2 = 1.5397$, $k_2 = 0.0083$, thickness of the adsorbate $d_2 = 0.575\text{ nm}$, $n_1 = 1$, $k_1 = 0$. Right panel: The transition dipole moment vectors of asymmetric and symmetric carboxylate vibrations.

in our experiment, the reflectivity difference of E_s and $E_{p,n}$ is negative, whereas it is positive for the $E_{p,t}$ component. As shown in Fig. 2, the sign of the $\nu_{as}(\text{OCO})$ mode at 1498 cm^{-1} is positive. This vibration can only be excited by the $E_{p,t}$ component via coupling to the TDM parallel to the surface, while the intense negative $\nu_s(\text{OCO})$ band at 1426 cm^{-1} results essentially from the interaction with $E_{p,n}$ via coupling to the TDM perpendicular to the surface.

Based on the above analysis of the IR data, we conclude that the BA molecule adsorbs dissociatively on the $\text{TiO}_2(110)$ surface. The resulting benzoate is proposed to be a bidentate species bound to surface Ti_{5c} atoms in an upright geometry. This conclusion is nicely corroborated by our DFT calculations and is consistent with the STM observation [8, 9]. The proton removed from the BA is transferred to a substrate O-atom, as evidenced by the OH band observed at 3700 cm^{-1} (Fig. 3). In accord with the theoretical calculations, this vibration is assigned to an H-atom bound to a surface bridging O_{2c} site. The frequency of this OH_{br} species is rather similar to that of hydroxyls formed on the same surface after exposure to atomic hydrogen [30] or after H_2O dissociation at surface O vacancies [31,32].

For submonolayer adsorption of BA, another OH band at slightly lower frequencies was detected at 3622 cm^{-1} (Fig. 3A–C). We can first rule out an assignment to hydroxyl group in BA molecule because of the lack of a $\nu(\text{C}=\text{O})$ band around 1700 cm^{-1} being characteristic for molecularly adsorbed BA. Furthermore, this band cannot be attributed to an OH species formed at surface O_{3c} sites. The O_{3c} atom is coordinatively saturated and is rather inactive for the interaction with hydrogen, in line with our DFT calculations. The 3622 cm^{-1} band might originate from the surface OH_{br} groups which are influenced by the modified local electronic structures (e.g. in the presence of subsurface defects) and/or by the weak interaction with adjacent benzoates. Further experimental and theoretical investigations are required to identify this isolated hydroxyl species.

Interestingly, at full monolayer coverage, the OH band at 3622 cm^{-1} disappears whereas the 3700 cm^{-1} band is still visible (Fig. 3D). This finding implies a change in the adsorption geometry of the benzoate species. Indeed, previous STM studies [8,9] revealed that dimerized benzoate species are formed at saturation coverage. The dimerization of benzoates is attributed to the attractive interaction between the phenyl rings along the $[1\bar{1}0]$ direction, where one phenyl ring is rotated around the molecular axis by 90° , thus allowing the interaction of hydrogen atoms with the π orbital of the neighboring benzoate. In this case, the benzoate species are stabilized by attractive intermolecular interaction forming T-shaped dimers across bridging O_{2c} rows.

We focus now on the interaction of terephthalic acid (TPA) with $\text{TiO}_2(110)$. At low coverage, the adsorption of TPA undergoes deprotonation forming carboxylate species, as confirmed by the observation of two IR bands at 1412 cm^{-1} ($\nu_s(\text{OCO})$) and 1635 cm^{-1} ($\nu_{as}(\text{OCO})$). The position of the $\nu_{as}(\text{OCO})$ mode, together with the relatively large frequency splitting (223 cm^{-1}) of the symmetric and asymmetric carboxylate stretch vibrations, suggests the presence of a monodentate configuration [33,34]. Furthermore, at low coverage, the spectra (Fig. 4A, B) do not show any $\nu(\text{C}=\text{O})$ bands at higher frequencies resulting from carbonyl in the carboxylic group. This finding reveals that both carboxylic groups in TPA are deprotonated giving rise to two carboxylate species per TPA. Importantly, an OH band was observed at 3700 cm^{-1} which is attributed to substrate hydroxyls formed through hydrogen transfer from TPA to bridging O_{2c} sites, as discussed above for the case of BA (Fig. 3).

Overall, the identification of monodentate carboxylate (instead of a bidentate one), together with the formation of OH species at surface O_{2c} sites, provides direct spectroscopic evidence for a flat-lying adsorption geometry of the dissociatively adsorbed TPA on $\text{TiO}_2(110)$, in excellent agreement with results obtained from NEXAFS and NC-AFM as well as from DFT calculations [13,16]. At low coverages, the adsorption of TPA on $\text{TiO}_2(110)$ occurs via deprotonation of both carboxyl groups

forming carboxylates bound to the surface Ti_{5c} sites in a monodentate fashion (see Fig. 1). Based on the flat-lying adsorption geometry, both $\nu_s(\text{OCO})$ and $\nu_{as}(\text{OCO})$ vibrations involve a main component of the TDM perpendicular to the surface, which couples to the p-polarized $E_{p,n}$ light. As a consequence, the corresponding IRRAS bands should be negative, as confirmed by the present IR spectra shown in Fig. 4A, B.

Upon increasing the TPA doses, the IR spectra change dramatically, indicating that the adsorption configuration of TPA molecules is coverage dependent. As shown in Fig. 4C, for higher coverages, the monodentate-related IR bands have disappeared completely. As in case of BA (see above), the new bands at 1427 and 1498 cm^{-1} are characteristic for a bidentate carboxylate and are assigned to $\nu_s(\text{OCO})$ and $\nu_{as}(\text{OCO})$, respectively. The sign of the $\nu_s(\text{OCO})$ band is negative whereas the $\nu_{as}(\text{OCO})$ one is positive. A closer analysis based on the reflectivity calculations displayed in Fig. 6B reveals a transition from flat-lying to upright configurations of TPA molecules on $\text{TiO}_2(110)$, where TPA is bound to the surface Ti_{5c} sites via a single bidentate carboxylate (Fig. 1). This configuration involves a “free” apical carboxylic group pointing away from the substrate, as supported by the observation of an additional $\nu(\text{C}=\text{O})$ band at 1760 cm^{-1} (Fig. 4C). In accord with our DFT calculation and the IR data for carboxylic acid monomers in Ar matrix [35], this band is assigned to carboxyl group in the top carboxylic acid. Simultaneously, in the OH stretching region a new band shows up at 3582 cm^{-1} (Fig. 5C). This vibration is characteristic for the OH group in the top carboxylic acid [35]. On the basis of the present IR results, the presence of TPA in a dianionic configuration, where the upper carboxylic group is also deprotonated, can be definitively ruled out. This conclusion is further supported by our DFT calculations. Interestingly, we see again an OH band at 3621 cm^{-1} , which in an analogous way is tentatively attributed to an additional surface hydroxyl species formed at bridging oxygen sites, as discussed above for the BA/ $\text{TiO}_2(110)$ system.

For TPA adsorption at full monolayer, the adsorbed carboxylate group remains in a bidentate fashion as demonstrated by the same $\text{C}=\text{O}$ stretching vibrations observed in Fig. 4D. However, a new carbonyl $\nu(\text{C}=\text{O})$ vibration is detected at 1690 cm^{-1} (Fig. 4D), while the OH band at 3582 cm^{-1} shows a clear decrease in intensity (Fig. 5D). These findings reveal a significant modification in the apical carboxylic group.

Recently, combined STM and DFT calculations [14–16] suggested that at saturation coverage, TPA molecules undergo dimerization on $\text{TiO}_2(110)$ via attractive intermolecular interactions within the monolayer. The TPA dimers prefer to adopt a plane-to-plane configuration with a C_2 local symmetry, where the TPA dimer is stabilized by the formation of double hydrogen bonds between the hydroxyl and carbonyl oxygen of both apical carboxylic groups. The dimerization is accompanied by mutual inclination and rotation of the adjacent TPA molecules in order to reduce repulsive interactions between the phenyl rings [16]. As a consequence, it is expected that both carbonyl $\nu(\text{C}=\text{O})$ and OH stretching vibrations shift to lower frequencies. Indeed, at full monolayer, the intensity of the OH band at 3582 cm^{-1} is significantly decreased. Note that due to broadening and intensity problems, the red-shifted OH band in the TPA dimers was not detected in the present IR spectra. The new carbonyl band at 1690 cm^{-1} (Fig. 5D) exhibits a red-shift by 70 cm^{-1} with respect to the one for the free carboxylic group. This band is characteristic for the carbonyl species in a cyclic dimer with double hydrogen bonds [36].

5. Conclusions

The adsorption of BA and TPA molecules on $\text{TiO}_2(110)$ at room temperature was studied systematically by IRRAS and DFT calculations. The high-quality IR data, in particular the observation of substrate hydroxyl bands, provide direct spectroscopic evidence for the formation of different adsorption configurations of BA and TPA depending on the coverage.

It was found that both molecules adsorb dissociatively on TiO₂(110) via deprotonation forming hydroxyls at bridging O_{2c} sites and carboxylate groups bound to the surface Ti_{5c} sites. At low coverages, the isolated benzoate adopts a bidentate fashion in an upright geometry, while the dissociatively adsorbed TPA molecule is bound to TiO₂(110) via both monodentate carboxylates in a flat-lying configuration. Further increasing the coverage of TPA leads to a conversion from flat-lying to upright-oriented molecules. At full monolayer adsorption of BA and TPA, dimerization occurs for both molecules due to attractive intermolecular interactions within the monolayer. The formation of BA dimers results from the interaction between adjacent phenyl rings, while the TPA dimers are stabilized by the formation of double hydrogen bonds between neighboring apical carboxylic groups.

Acknowledgements

M. Buchholz gratefully acknowledges the financial support from the Helmholtz Research School “Energy-Related Catalysis”.

References

- [1] A. Fujishima, K. Honda, *Nature* 238 (1972) 37.
- [2] T.L. Thompson, J.T. Yates, *Chem. Rev.* 106 (2006) 4428.
- [3] B. O'Regan, M. Grätzel, *Nature* 353 (1991) 737.
- [4] M. Grätzel, *Nature* 414 (1991) 338.
- [5] M. Grätzel, *J. Photochem. Photobiol. C* 4 (2003) 145.
- [6] U. Diebold, *Surf. Sci. Rep.* 48 (2003) 53.
- [7] M.C. Xu, H. Noei, K. Fink, M. Muhler, Y.M. Wang, C. Wöll, *Angew. Chem. Int. Ed.* 51 (2012) 4731.
- [8] Q. Guo, I. Cocks, E.M. Williams, *Surf. Sci.* 393 (1997) 1.
- [9] Q. Guo, E.M. Williams, *Surf. Sci.* 433–435 (1999) 322.
- [10] J. Schnadt, J. Schiessling, J.N. O'Shea, S.M. Gray, L. Patthey, M.K.J. Johansson, M. Shi, J. Krempaský, J. Åhlund, P.G. Karlsson, P. Persson, N. Mårtensson, P.A. Brühwiler, *Surf. Sci.* 540 (2003) 39.
- [11] J. Schnadt, J.N. O'Shea, L. Patthey, J. Schiessling, J. Krempaský, M. Shi, N. Mårtensson, P.A. Brühwiler, *Surf. Sci.* 544 (2003) 74.
- [12] D.G. Grinter, C.L. Pang, C.A. Muryn, F. Maccherozzi, S.S. Dhesi, G. Thornton, *J. Phys. Chem. Lett.* 5 (2014) 4265.
- [13] P. Rahe, M. Nimmrich, A. Nefedov, M. Naboka, C. Wöll, A. Kühnle, *J. Phys. Chem. C* 113 (2009) 17471.
- [14] A. Tekiel, J.S. Prauzner-Bechcicki, S. Godlewski, J. Budzioch, M. Szymonski, *J. Phys. Chem. C* 112 (2008) 12606.
- [15] J.S. Prauzner-Bechcicki, S. Godlewski, A. Tekiel, P. Cyganik, J. Budzioch, M. Szymonski, *J. Phys. Chem. C* 113 (2009) 9309.
- [16] F. Zasada, W. Piskorz, S. Godlewski, J.S. Prauzner-Bechcicki, A. Tekiel, J. Budzioch, P. Cyganik, M. Szymonski, Z. Sojka, *J. Phys. Chem. C* 115 (2011) 4134.
- [17] Y. Wang, A. Glenz, M. Muhler, C. Wöll, *Rev. Sci. Instrum.* 80 (2009) (113108–113106).
- [18] W.N. Hansen, *J. Opt. Soc. Am.* 58 (1968) 380.
- [19] W.N. Hansen, *Symp. Faraday Soc.* 4 (1970) 27.
- [20] J.A. Mielczarski, R.H. Yoon, *J. Phys. Chem.* 93 (1989) 2034.
- [21] M. Buchholz, P.G. Weidler, F. Bebensee, A. Nefedov, C. Wöll, *Phys. Chem. Chem. Phys.* 16 (2014) 1672.
- [22] G. Kresse, J. Furthmüller, *Phys. Rev. B* 54 (1996) 11169.
- [23] G. Kresse, D. Joubert, *Phys. Rev. B* 59 (1999) 1758.
- [24] J.P. Perdew, K. Burke, M. Ernzerhof, *Phys. Rev. Lett.* 78 (1997) 1396–1396.
- [25] P.E. Blöchl, *Phys. Rev. B* 50 (1994) 17953.
- [26] Y. Kim, K. Machida, *Spectrochim. Acta A* 42 (1986) 881.
- [27] G. Varsanyi, *Assignment for Vibrational Spectra of Seven Hundred Benzene Derivatives*, Adam Hilger, London, 1974.
- [28] C.A. Tellez, E. Hollauer, M.A. Mondragon, V.M. Castano, *Spectrochim. Acta A* 57 (2001) 993.
- [29] M.C. Xu, Y.K. Gao, Y. Wang, C. Wöll, *Phys. Chem. Chem. Phys.* 12 (2010) 3649.
- [30] X.L. Yin, M. Calatayud, H. Qiu, Y. Wang, A. Birkner, C. Minot, C. Wöll, *ChemPhysChem* 9 (2008) 253.
- [31] M.A. Henderson, *Surf. Sci. Rep.* 46 (2002) 1.
- [32] M.A. Henderson, W.S. Epling, C.H.F. Peden, C.L. Perkins, *J. Phys. Chem. B* 107 (2003) 534.
- [33] M.C. Xu, H. Noei, M. Buchholz, M. Muhler, C. Wöll, Y. Wang, *Catal. Today* 182 (2012) 12.
- [34] M. Buchholz, Q. Li, H. Noei, A. Nefedov, Y. Wang, M. Muhler, K. Fink, C. Wöll, *Top. Catal.* 58 (2015) 174.
- [35] S.G. Stepanian, I.D. Reva, E.D. Radchenko, G.G. Sheina, *Vib. Spectrosc.* 11 (1996) 123.
- [36] R. Arnold, W. Azzam, A. Terfort, C. Wöll, *Langmuir* 18 (2002) 3980.